Int. J. Electrochem. Sci., 11 **(2016)** 763 - 776

International Journal of
ELECTROCHEMICAL
SCIENCE
www.electrochemsci.org

Selective and Sensitive Electrochemical DNA Biosensor for the Detection of *Bacillus anthracis*

Mukhil Raveendran[1], *Ana F. B. Andrade*[1,2], *Jose Gonzalez-Rodriguez*[2,*]

[1] School of Chemistry, University of Lincoln, Brayford Pool, Lincoln LN6 7TS, UK.
[2] Criminalistic Intitute, Federal District Civil Police, SPO, lote 23, bloco A, subsolo, Brasilia, DF, Brazil
[*]E-mail: jgonzalezrodriguez@lincoln.ac.uk

Received: 31 October 2015 / *Accepted:* 19 November 2015 / *Published:* 1 December 2015

The development of a selective and sensitive electrochemical DNA biosensor for detection of the pathogen *Bacillus anthracis* is proposed here. The technique is based on the characteristic cyclic voltammetry (CV) redox peaks and the very selective nature of DNA hybridization. The designed system consists of a self-assembled layer of mercaptohexanol (MCH) and thiol linked probe (ssDNA-thiol) immobilized on gold-modified screen-printed electrodes. This direct detection technique studies the change in potential and intensity of the surface-modified screen-printed electrodes when a 5mM $Fe(CN)_6^{3-}$ solution in 0.1M KClis presented to the electrodic system in the range between -0.5 to 0.7V. The increase or decrease in the electron transfer along with the varied redox potential during immobilization of the probe and hybridization of the target was observed as CV peak current and potential change. The proposed system showed reliable results with sensitivity up to 10pM and selective enough to distinguish signals from DNA fragments presenting 1bp mismatches. The fabricated system with the thiol probe once produced could be shelved for 2-3 months.Thus the strong selective binding nature of the DNA along with the sensitive CV characters, prove to be an efficient system for reliable detection of pathogens.

Keywords: Bacillus anthracis, DNA biosensor, Cyclic voltammetry, bioweapons, bioelectrochemistry

1. INTRODUCTION

Electrochemical techniques integrating bio-molecules for biological applications are a fast developing area with multiple applications in natural sciences. Over the years this interdisciplinary technique of designing detection systems for various purposes including pathogen detection, targeted cancer therapy, environmental screening systems, tools for medico-clinical usage, etc. are gaining steadfast progression [1]. Amongst different electrochemical sensors, those exploiting DNA probes for

detecting microbes via DNA-DNA hybridization are being studied extensively in many fields. Main reasons being simple design, high sensitivity, low cost, micro fabrication possibilities, and likely miniaturization of the detecting system. The very nature of DNA to recognise and hybridise complementary nucleotide sequences makes DNA biosensor a very promising domain.

Attempts to enhance DNA biosensors technology to be used for on-field detection with high reliability have greatly helped improve various aspects of this detecting system. Use of gold for DNA attachment through a thiol group has been extensively used due to its ability to efficiently conduct and amplify electrochemical signals while retaining biological activity [2-4]. The strong binding nature of gold to any thiol group makes it desirable for biosensor assembly [5-7].

Within the main factors impacting on sensor performance, optimum surface density of DNA probes has been reported as an important one for successful detection. Mercaptohexanol (MCH) has been used to backfill electrodes after probe immobilization [8] in order to control non-specific interactions, allowing regulating DNA surface density through incubation time. Steel et al. (2000) [9] also analysed the length of the DNA probe as a contributing factor. Co-immobilization of DNA probes with a thiol spacer have also been reported to positivelymodify the surface and affecting the DNA probe density [10]. Alternative approaches used reductive de-absorption of mercaptoproionic acid (MPA) in a mixed MPA/MCH monolayer to immobilize single stranded DNA probes (ssDNA) onto gold [11]

Bacillus anthracis, a gram-positive spore forming bacterium has been a serious threat to the community as a bioweapon. Of the different routes of infection (cutaneous, gastrointestinal or respiratory), aerial dispersal of the deadly human anthrax bacteria has been proved fatal and is the most tailored form of bio hazardous agent [12-14]. Inadequate measures and incapacity for quick detection of anthrax spread terror and has claimed numerous lives in the past [15-17]. Usual methods for anthrax identification involve standard biological tests in the lab such as microbial culturing, immunological and serological tests, DNA typing and PCR methods that are time consuming and expensive [18,19]. Need for a fast and robust detection technique that could be used to detect presence of harmful microbes instantly has led to the growth of biosensor systems [20, 21].

Diverse research in this field has led to the development of many distinctive types of detecting systems. Nanomaterial based biosensors have been used due to its many unique electrical, magnetic and optical characteristics. Its small size and high surface area also support probe attachment and surface modifications [22]. Sequence specific Nanopore biosensor for detecting lethal factor in anthrax toxin has been recently developed. Using ionic modulation of the analytes and the residence time of the analyte coupled with amplitude blockade events, Wang et al [23] were able to detect the target analyte and measure its concentration. Likewise, Pal & Alocilja [24] described an electrochemical transducer utilizing electrically active magnetic nanoparticles. Optical biosensors using fiber optic waveguide and peptide integrated ligands for anthrax spore detection have also been used [25]. Anthrax spore detection in liquids attempted using the sensitive Love wave sensor (surface acoustic wave sensor) by screening waveguides was published by Branch &Brozik [26].

With innovative sensors easing into the field of diagnostics and screening, an effective detection system for timely response and prevention before infection is yet to be perfected. Though

countable research articles on biosensors for anthrax detection have been previously published further research is still needed.

Though many successful electrochemical DNA biosensors with or without employing self-assembled monolayer have been already published [21], [27-30]. In this paper, we propose DOE as a method to statistically estimate optimum MCH-ssDNA/thiol concentrations to achieve reasonable surface coverage so as to improve signal detection. Usage of gold electrodeposited carbon screen-printed electrode for MCH-ssDNA/thiol attachment aimed at successful detection of *B.anthracis* specific DNA sequences has been also attained through this paper.

2. MATERIALS AND METHODS

2.1. Instruments

The cyclic voltammetry (CV) were performed with an Autolab III (Methrom, Switzerland) potentiostat/galvanostat and controlled by Autolab GPES software version 4.9 forWindows XP. Electrochemical measurement were performed using carbon screen-printed electrodes with a 3mm working area, purchased from Dropsense (Oviedo, Spain).

2.2. Chemicals

Analytical grade reagents were used as received without any additional purification from Sigma-Aldrich (Gillingham, UK). Deionised water (resistivity > 16 MΩ cm) was used throughout the experiments to prepare all solutions.

2.3. Pretreatment of SPE

Carbon screen-printed electrodes were cleaned to remove any surface impurities and to obtain a suitable surface for electrodeposition. The pretreatment procedure consisted in apply a potential of +1.6V for 120 s and +1.8V for 60 s in 0.25M acetate buffer containing 1mM KCl (pH 4.75) with constant stirring. This was followed by 10 cycles between 0 and +1.4V in 0.1mol per liter glycine (pH 2.0) as described previously by Pereira et al. [31] and Regiard et al [32]. The etched carbon surface provided uniform and stable gold coverage. The procedure also assured reproducible voltammograms.

2.4. Electrodeposition of Gold onto carbon SPE

The procedure for gold electroplating/electrodepositing was redesigned from several successful papers [31], [33,34]. The pretreated carbon SPE was immersed into 0.25 mM $HAuCl_4$ solutions containing 0.1M KNO_3 prepared with doubly distilled water, and de-aerated by bubbling with nitrogen. A constant potential of -0.2 V was applied for 300 seconds. The number of cycles required

for proper gold coverage depended on the $HAuCl_4$ solution concentration. Above mentioned concentrations achieved complete and stable coverage at 6 - 10 cycles and hence considered optimum. It should be noted that too high Au concentrations resulted in quick deposition but unstable coverage. Successful deposition was observed both physically and electrochemically by cyclic voltammetry by running $Fe(CN)_6^{3-}$ in 0.1 M KCl as electrolyte. The gold electrodes were checked for reproducible voltammograms by calculating standard deviation from the peak area and peak heights. Figure 1 shows the standard cyclic voltammogram for gold electrode in 5mM $Fe(CN)_6^{3-}$ in 0.1M KCl. The modified electrode washed with doubly distilled water (dried with nitrogen) was carefully stored in dark airtight containers for further use.

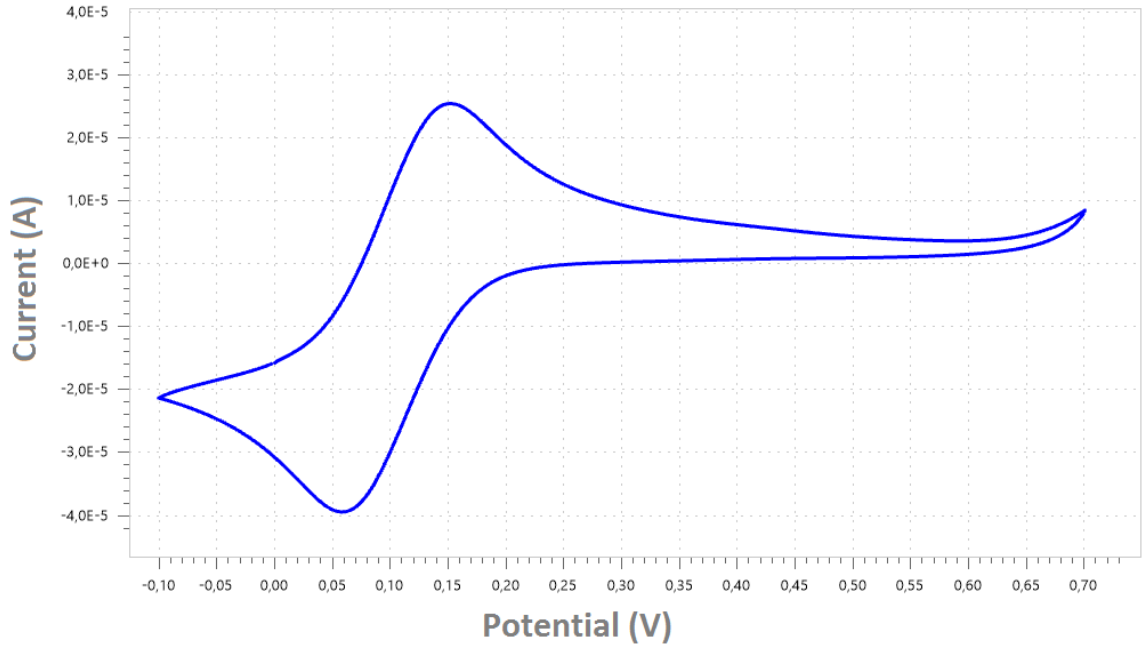

Figure 1. Cyclic voltammetry of Gold deposited Carbon SPE, 10 repetitions resulted in an average peak height - $2.82x10^{-05}$ A and peak position of - 0.261V.

2.5. Probe and target sequence selection

A 20bp unique sequence from the proactive antigen gene (pag gene ID 3361714) in pXO1 plasmid of *Bacillus anthracis* [35] was selected as the target sequence. Sequence was present in several recently sequenced *B. anthracis* strains in GenBank. The specific sequence flanked with Pst1 restriction sites allowed easy access for detection and for any other molecular or genetic analysis. The probe sequence (30bp) was designed complementary to the target with an additional 10bp and thiol linker at the 5' end (ssDNA thiol). Target sequences with 1bp, 2bp, 3bp mismatches were also designed (as shown in table 1) to check the selectivity of the probe-target binding and strength of the electrochemical cyclic voltammograms. A completely random sequence was also designed as a negative control to assess the selectivity and cross-reactivity of the target sequence.

Table 1. DNA sequences used as probe, target and mismatch in this study.

	Sequence
Thiol modified probe sequence	5'- HS- $(CH_2)_6$ – AGTCTTCGGCACGAGGTAAAAAGTCCTCTA- 3'
Target sequence	5'-TAGAGGACTTTTTACCTCGT -3'
1 bp mismatch	5'TAGAGGTCTTTTTACCTCGT 3'
2 bp mismatch	5'TAGAGGTGTTTTTACCTCGT 3'
3 bp mismatch	5'TAGAGGTGGTTTTACCTCGT 3'
Negative control	5'GTTCCCTTAGCAGCTAGCTA 3'

2.6. Immobilization and hybridization of probe and target DNA:

All probe and target sequences were obtained from Sigma Aldrich (UK) and double-checked for purity and concentration after dilution using the Nanodrop spectrophotometer. The ssDNA linked probe sequence in disulfide (S-S) form was cleaved using a NAP 10 column with 0.01M sodium phosphate as equilibrant.

The concentration of both mercaptohexanol (MCH) and the probe (ssDNA Thiol) were optimised using design of experiments and an ANOVA model. A 3-level factorial design: 3^2 design studying the effects of 2 factors in 10 runs was created. The design was run in a single block. The order of the experiments was fully randomized to provide protection against the effects of lurking variables.

Prior to probe immobilization, the gold deposited electrodes were immersed in an optimum concentration of mercaptohexanol (MCH) for 1 hour. The electrodes were then washed with phosphate buffer (pH 7.4) and distilled water [8, 36].Use of MCH as a self-assembled monolayer assured spacing between the thiol linked probes and enhanced target hybridization.

Immobilization of ssDNA thiol probe onto gold was achieved by placing 2.0 µl of the probe DNA on the electrode and incubating it at 30°C for 60 minutes [7]. After incubation the electrode was rinsed thoroughly with 10 mM phosphate buffer (pH 7.4) followed by distilled water. Successful immobilization was followed by hybridization of target DNA, this was achieved by incubating the probe anchored electrodes with 2.0 µl of target DNA at 37°c for 60 minutes. The electrodes were finally washed with Phosphate Buffer (7.4 pH) and distilled water.

Positive immobilization and detection of target sequence was confirmed by characterizing the electrode in 5mM $Fe(CN)_6^{3-}$ with 0.1M KCl as electrolyte. The shift in the cyclic voltammograms was used to identify probe anchoring and target detection.

3. RESULTS AND DISCUSSION

3.1. Optimization of MCH and and thiol concentration

Sulfur comprising compounds (like MCH) with both thiol and carboxylic acid groups have been identified suitable for biosensor design. The thiol group acts as a link for metallic attachments providing stable monolayers. It has also been evidenced that the carboxylic acid groups react covalently with phosphate backbone of DNA thus achieving effective immobilization and stability [37-40]. The presence of MCH as a spacer thiol prevents the ssDNA from adhering to Au through their nitrogenous bases. This ensures that all the ssDNA is anchored onto the gold surface only by the thiol end. MCH also helps to achieve better hybridization by reducing steric and electrostatic hindrances occurring due to tightly packed probe DNA monolayer [8].

Therefore the concentration of self-assembled layer of MCH anchored on the metallic surface (gold) plays an important role in attaining decent target identification signal. The amount of MCH molecules regulates ssDNA-thiol probe anchoring and exposure of the probes for hybridization with target sequences. This in turn controls the shift in peak current and potential needed for target detection. Hence it was important to find an optimal MCH and ssDNA-thiol concentration that presented with maximum peak shift on immobilization that in turn increases peak-to-peak shift upon hybridization. While incubation time [41] and mole ratio of DNA [10] have been utilized to control the surface density of DNA, we used Design of Experiments (DOE) to calculate the optimal concentration for the system MCH/ssDNA-thiol in order to obtain an optimal peak current and potential difference on hybridization. The response surface design with different ssDNA-thiol and MCH concentrations as experimental factors was carried out.

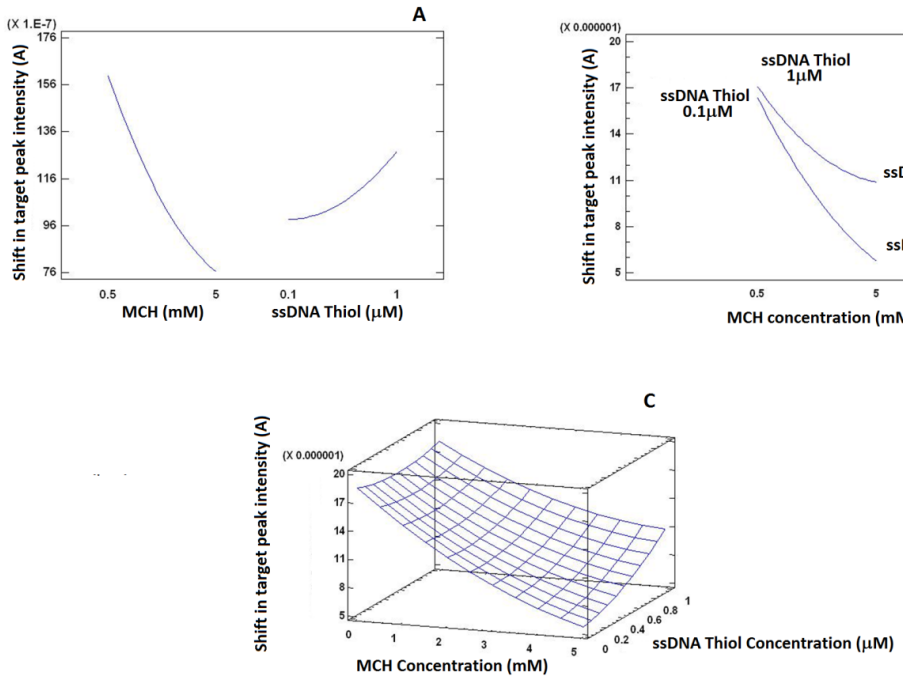

Figure 3. Influence of the MCH and Thiol concentration in the peak current. (A) individual concentration effects, (B) Interaction plot and (C) Estimated response surface.

The ANOVA test produced a theoretical model that fitted at 100% the experimental data for a shift in peak current and 68.7% for shifts in peak potential,at 95% confidence level. Both MCH concentration and ssDNA-thiol concentration seemed to have an effect on peak current individually, as visually plotted in the individual (Figure 3A) and main effects plot (Figure 3B). There is no interaction between variables and it is evident from these plots that peak current decreases with increase in MCH concentration. It was also noted that at low concentrations of MCH, an increase in the probe concentration [ssDNA Thiol] did not affect immobilization peak current shift significantly. The shift was significant when high MCH concentration and high probe concentration was used. However, as seen in Figure 3B, in order to maximize the signal low MCH concentrations were selected as this value for the variable produces the maximum shift to increase sensitivity

Figure 3C shows the surface response for the shift in the intensity and it can be observed that at minimum MCH concentration the ssDNA thiol concentration to obtain maximum signal can be kept a low levels. The surface fits the equation:

Anodic Peak current Shift = $1.8458x10^{-5}$ - $3.7760x10^{-6}$[MCH]- $3.6455x10^{-6}$[ssDNA-thiol] + $2.3986x10^{-7}$[MCH]^2 + $1.0864x10^{-6}$[MCH][ssDNA-thiol] + $3.5273x10^{-6}$[ssDNA-thiol]^2

The shift in potential was also a subject to DoE. As shown in Figure 4A, an increase in the concentration of MCH and ssDNA thiol produced an increase and a decrease of the shift potential respectively. The interaction plot shown in Figure 4B also shows how the lower values in MCH concentration offered the highest values in shift potentials (highest at the bottom of the scale) specially at lower ssDNA thiol concentrations.

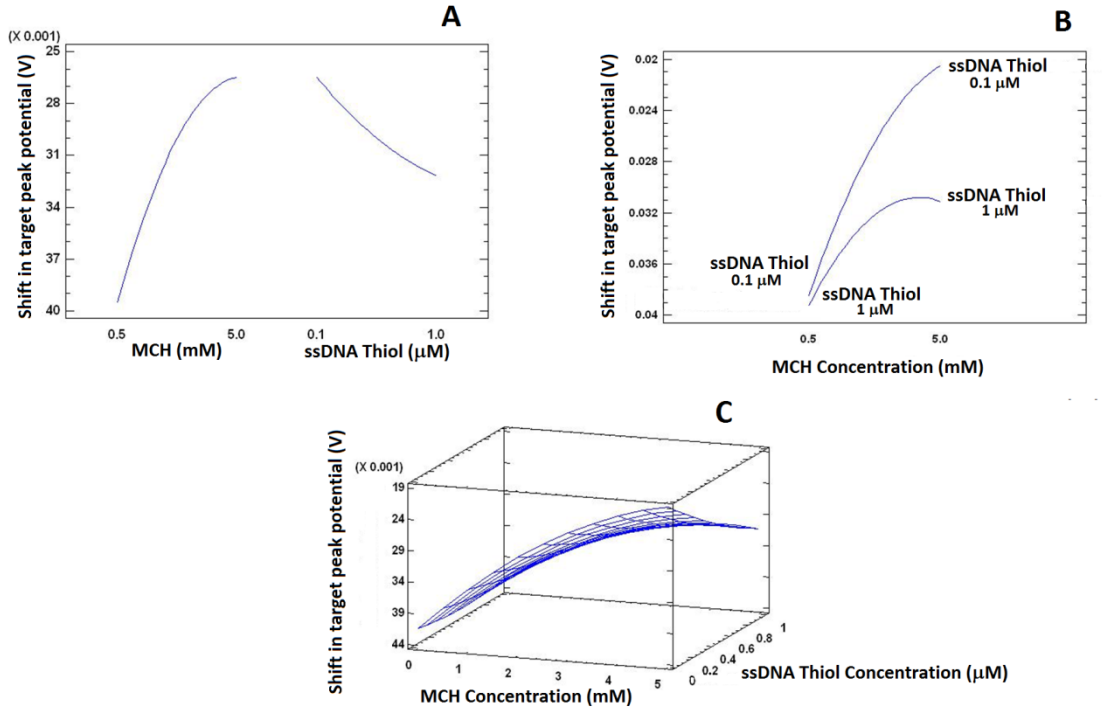

Figure 4. Influence of the MCH and Thiol concentration in the position of the target peak position. (A) Concentration effects, (B) Interaction plot and (C) Estimated response surface.

Figure 4C shows the surface response for the system and how maximum shift in target peak potential is achieved at high MCH and low ssDNA Thiol concentrations, respectively.

The equation of the surface response is:

Anodic peak voltage Shift = $-4.1616\text{x}10^{-2} + 7.4846\text{x}10^{-3}$[MCH] - 3.2696x10-3[ssDNA-thiol] - $5.9359\text{x}10^{-4}$[MCH]^2 - $2.4114\text{x}10^{-3}$[MCH][ssDNA-thiol] + $3.2466\text{x}10^{-3}$[ssDNA-thiol] ^{2}

Taking all these factors into account DOE estimated a combination of 0.5 mM MCH concentration and 1.0 µM ssDNA-thiol concentration to be optimal towards achieving maximum yet stable anodic peak current and peak potential shift. MCH concentration seemed to offer the most important effect affecting both potential and intensity shifts.

Under these conditions the analysis on the change in the anodic peak current and peak voltage of the system MCH, thiol DNA probes and target sequence was studied. Figure 2 shows the CV voltammograms of the gold deposited electrode at these different stages. The shift in anodic peak current and voltage represents the difference in electron transfer and the change in redox potential between the gold surface and Fe(CN)6 3-/4-.

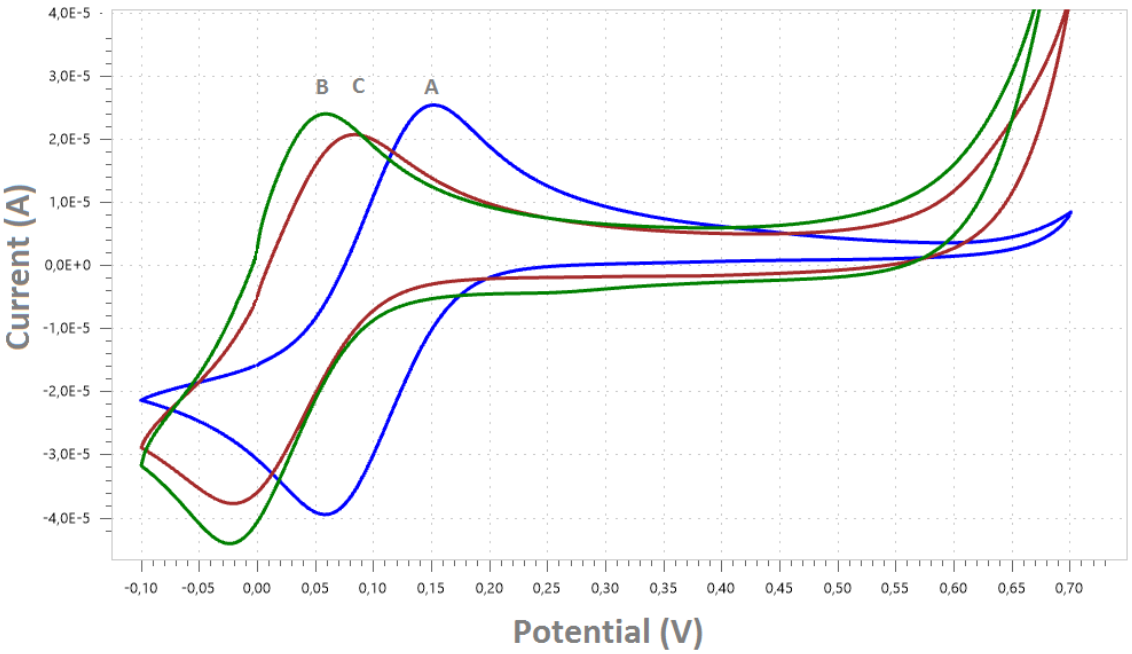

Figure 5. CV Voltammogram of 5mM $K_3Fe(CN)_6$ in a 0.1 KCl aqueous solution at (A) a gold deposited bare SPE, (B) a MCH/ssDNA-thiol linked SPE and (C) a target hybridized DNA SPE

The voltammogram obtained for $K_3Fe(CN)_6$ at the gold-modified carbon SPE can be observed in figure 5(A), showing a well-defined curve with average anodic peak current of $3.17\text{x}10^{-5}$ A. After the immobilization of the MCH and ssDNA-thiol the voltammogram for the $K_3Fe(CN)_6$ exhibited a decrease in peak current to $1.84\text{x}10^{-5}$A, followed by further decrease to 9.08x10-^{6} A upon target hybridization. This seems to indicate that the anodic peak current seemed to decrease with immobilization and hybridization. The voltage for the anodic peak of $K_3Fe(CN)_6$ was 0.138 V and

shifted to more negative values when analysed with the MCH/ssDNA-thiol modified SPE (0.036 V), reverting to more positive potentials (0.069V) upon hybridization of the anthrax DNA.

The explanation for this behavior lies on the negatively charged nature of DNA and the transfer of electrons during the hybridization event. The gold surface will transfer the electrons from the $Fe(CN)_6^{-3}$ and viceversa during cyclic voltammetry to produce the characteristic voltammogram at the specified voltage. Modification of the gold surface by the MCH and the ssDNA-thiol will modify this transfer of electrons reducing the potential at which this is occurring, making it easier for the thiocyanate to reduce. During the hybridization of the anthrax DNA with the complementary strain of the ssDNA-thiol immobilized on the surface there is a restructuration of the molecules and a higher demand for electrons for the formation of the dsDNA, which modifies the potential at which the thiocyanate ion will reduce with less electrons available for the molecule, hence increasing the reduction potential.

3.2. Bacillus anthracis detection

Identification of *Bacillus anthracis* was successfully achieved by detecting the change in anodic peak current and potential due to the direct binding of target DNA sequence to the immobilized probe DNA via complimentary strand hybridization. The decreased anodic peak current could be explained from the hypothesis that the MCH/ssDNA-Thiol layer on the gold surface creates a repulsion between $Fe(CN)6^{-3}$ and the negatively charged phosphate backbone of DNA to gold thus restricting electron transfer [42]. This results in a decreased anodic peak current. Further decrease in peak current is presumed as a result of DNA-DNA hybridization, an additional surface modification restricting electron flow and lowering peak current value. These results were in agreement with findings reported in the literature [7, 30, 43] and with many more extensively studied electrochemical analyses using peak current change to identify biomolecules directly and indirectly [29, 32, 44, 45]. Also studies involving redox reactions of DNA [42] suggest that the decrease in peak current after hybridization might be due to the difficulty in oxidizing duplex form of DNA, as a result of hydrogen bond formation between the ssDNA probe and target strands.

An interesting outcome in our study is the consistent peak voltage shift upon immobilization and hybridization. Different authors in the literature [7, 30, 43] speak about the increase in peak voltage upon ssDNA monolayer linkage and target DNA binding on different modified surfaces of gold and glassy carbon electrode. Serpi et al [46], reported a decrease in peak voltage separation with surface modified carbon nanotube paste electrode. Whilst all of the aforementioned papers used change in peak current, none of them use peak potential shift directly to detect DNA.

The steady and consistent decrease and increase of peak potential upon immobilization and hybridization respectively could also be used as a parameter for target detection. Figure 6 shows the different peak potentials for the numerous tested SPEs upon ssDNA-thiol anchoring and target binding with specified uncertainties.

Even though the immobilization and hybridization peak currents and potentials seem to vary from electrode to electrode, the peak-to-peak separation was always significant enough (at 99%) to

detect probe immobilization and target hybridization. This variation could be related to the quantity of gold deposited on the carbon electrode influencing the available surface for DNA attachment.

To test this effect, the peak currents of Au deposited SPE were normalized with the quantity of gold deposited, measured by X-ray Fluorescence; the resultant normalized peak current values were consistent with all the electrodes indicating that concentration of gold did affect electron transfer. (Table 2).

Table 2. Normalization with respect to deposited Au concentration.

Screen Printed Electrodes	AU (ppm)	Actual Peak current	Normalized Peak current
1	902.32	3.64E-05	4.03E-03
2	699.22	2.82E-05	4.03E-03
3	849.54	3.43E-05	4.04E-03
4	793.63	3.20E-05	4.03E-03
5	688.12	2.77E-05	4.03E-03

3.3. Uncertainty

The gold electrodes were checked for reproducible voltammograms by calculating (3σ) standard deviation with 99% significance for the peak current and peak potentials.

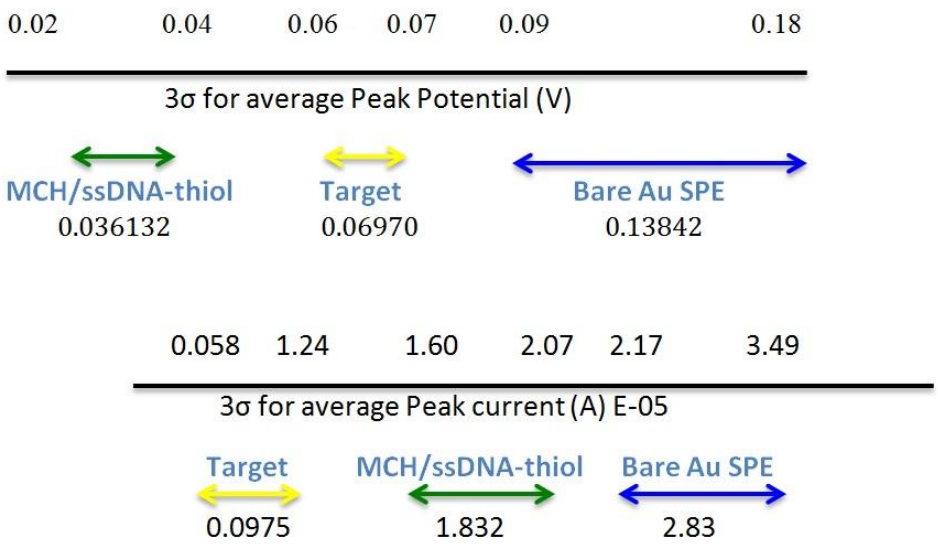

Figure 6. Uncertainty calculation - (3σ) standard deviation with 99% significance.

As different SPEs produced slightly different peak currents and voltages with respect to gold concentration it was essential to ensure that the peak-to-peak differences were still a reliable indication of DNA detection. Figure 6 shows the 3σ values above and below the average anodic peak potential

and current. It is clear from the readings that the thiocyanate values for the gold SPE, immobilised DNA-thiol and DNA hybridization events do not significantly overlap. The shift was always significant enough to differentiate and detect immobilization and hybridization.

3.4. Effect of target concentration on Anodic Peak current

Increased target DNA concentration was found linear showing a decrease in the anodic peak current. Keeping the optimal MCH-Thiol (0.5mM and 1.0μM) concentration constant, target concentrations were increased from 100pM to 2μM. The calibration curve showed a regression coefficient (r^2) of 0.9857. As more and more target DNA gets hybridized, the electron transfer gets restricted further and hence the weak anodic peak current signal. This further adds on to the theory that surface modification prevents free flow of electrons resulting in a lower anodic peak current value. Target concentrations did not have any significant effect on peak potentials shifts.

3.5. Limit of Detection and quantification

The anthrax DNA detecting system showed consistent results to low concentrations of DNA. Different target anthrax DNA concentrations were tested to calculate the detection and quantitation limits. Sensitivity of the system was found to be 10 pM.

3.6. Specificity of the detecting system

To assess the specificity of the detecting system, target anthrax DNA sequences with 1bp, 2bp, 3bp mismatches from the original one, and a DNA random sequence containing no similar pair of bases were tested. The gold deposited electrode was subjected to the same immobilization and hybridization procedure and electrochemical parameters for the mismatches. The CV voltammograms of these mismatches showed no significant change in anodic peak current and potential after hybridization, which means that no hybridization event was detected. Figure 7 shows the peak-to-peak current shift after hybridization for all the mismatches and the actual target. No overlap is observed between the error bars for the actual target and any potential cross-reaction with other DNA sequences, which implies significantly different results at 99%.

It is noticeable that 1bp mismatch shows a slight shift and the shift diminishes to nothing for the random sequence. It was also observed as the number of mismatched base pairs increased the shift became minimal. The Peak potential for the 1 bp-mismatched sequence gave a slight yet detectable signal; the voltage shifts for 2bp, 3bp and negative mismatches were not significant. Figure 8 shows that the mismatched bases gave very low potential shifts when compared to the target DNA sequence and yet significantly different to the target sequence (99% significance)

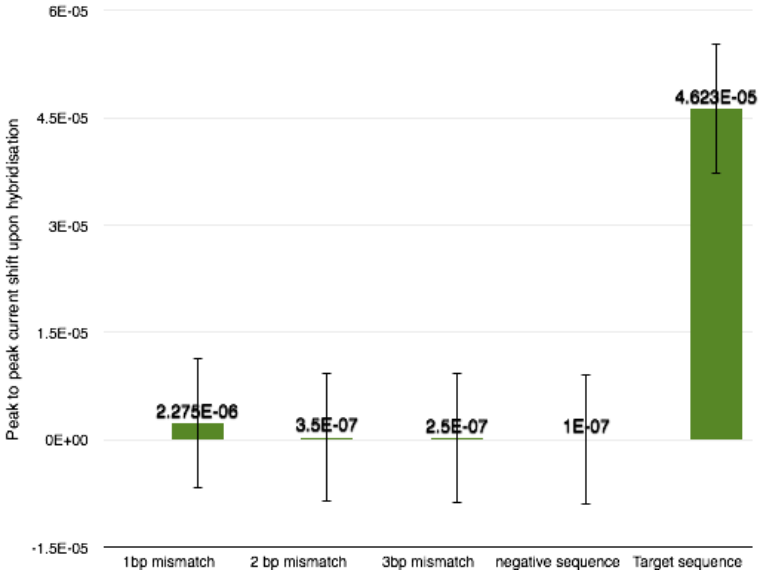

Figure 7. Error graph of hybridization peak current shifts with 1bp, 2bp, 3bp mismatches and random sequence (99% significance).

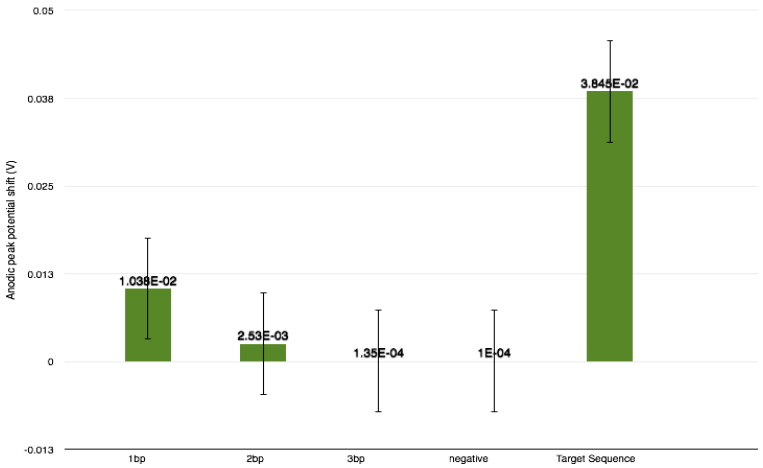

Figure 8. Error graph of hybridization Peak potential shifts with 1bp, 2bp, 3bp mismatches and random sequence (99% significance).

This could be explained by the theory that complementary DNA strands form a tightly packed duplex, and mismatched base pairs do not fit well into this tight binding site. Hence even though there is some binding between the probe and mismatched DNA, the mismatches weaken the binding and as the number of mismatched bps increase the peak current shift diminishes greatly.

4. CONCLUSION

A reliable electrochemical detection system for the bacterium *Bacillus anthracis* in liquid samples has been successfully demonstrated in this work. Gold deposited carbon screen-printed

electrodes effectively modified with a self-assembled monolayer of MCH have proved efficient for ssDNA-thiol probe anchoring. We further confirmed that controlling the concentration of MCH proves vital for better signal detection and influences probe immobilization and target hybridization. Consequently optimizing MCH and ssDNA-thiol concentrations is paramount; statistical analysis (DOE) was used to estimate an ideal value for attaining maximum peak current and potential shifts. DOE provided influence and significance of each factor (MCH and ssDNA-thiol concentration) and their effect on the response (peak current and peak potential) with agreeable r^2 values of 100% and 68.70% respectively. A concentration of 0.5mM for MCH and 1.0 μM for ssDNA-thiol probe was predicted as optimum.

SPEs designed with the above said optimal conditions were capable of producing well-defined Cyclic Voltammograms upon MCH/ssDNA-thiol immobilization and target hybridization. The observed shift in peak current and potential were employed for detecting target DNA. The peak shifts were found to be always consistent and significant to identify even the smallest mismatches in target DNA sequence, this was ascertained by uncertainty analyses. Selectivity studies indicated the system detected 1bp, 2bp, 3bp mismatched DNA and random sequences accurately. The detection system is sensitive enough to detect DNA samples as low as 10 pM and identifying *Bacillus anthracis* DNA using peak current and peak potential shifts respectively.

These results will also be beneficial to further develop and perfect detecting systems capable of detecting on scene samples efficiently. We also conclude, this system adaptable for detecting numerous other microbial threats, with refinement will be advantageous in many fields.

ACKNOWLEDGEMENTS
The authors are thankful to Policia Civil do Distrito Federal (PCDF), Fundação de Peritos em Criminalística Ilaraine Acácio Arce (FPCIAA) and Fundação de Apoio a Pesquisa do Federal (FAP-DF) for the financial support.

References

1. J. Gonzalez-Rodriguez, M. Raveendran, *Biosensors Journal*, 4 (1) (2015) 1
2. B. Elsholz, A. Nitsche, J. Achenbach, H. Ellerbrok, L. Blohm, J. Albers, G. Pauli, R. Hintsche, R. Wörl, *Biosens. Bioelectron*., 24 (2009) 1737
3. F. Li, Y. Feng, P. Dong, B. Tang, *Biosens Bioelectron.*, 25 (2010) 2084.
4. G. Martínez-Paredes, M.B. González-García, A. Costa-García, *Sensors Actuators, B Chem.*, 149 (2010) 329
5. C.D. Bain, E.B. Troughton, Y.T. Tao, J. Evall, G.M. Whitesides, R.G. Nuzzo, *J. Am. Chem. Soc.*, 111 (1989) 321.
6. A. Ulman, *Chem. Rev.*, 96 (1996) 1533.
7. R. Das, A.K. Goel, M.K. Sharma, S. Upadhyay, *Biosens. Bioelectron.*, 74 (2015) 939
8. T.M. Herne, M.J. Tarlov, *J. Am. Chem. Soc*., 119 (1997) 8916
9. A. B. Steel, R.L. Levicky, T.M. Herne, M.J. Tarlov, *Biophys. J*., 79 (2000) 975
10. S.D. Keighley, P. Li, P. Estrela, P. Migliorato, *Biosens. Bioelectron.*, 23 (2008) 1291
11. M. Satjapipat, R. Sanedrin, F. Zhou, *Langmuir*., 17 (2001) 7637
12. T. Dixon, M. Meselson, J. Guillemin, P. Hanna, *New Engl. J. Med.*, 341 (1999) 815
13. E. D'Amelio, B. Gentile, F. Lista, R. D'Amelio, *Environ. Int.*, 85 (2015) 133
14. A.K. Goel, *World J. Clin. Cases*, 3 (2015) 20
15. B. A. Perkins, T. Popovic, K. Yeskey, *Emerg. Infect. Dis.*, 8 (2002) 1015

16. D.B. Jernigan, P.L. Raghunathan, B.P. Bell, R. Brechner, E. A. Bresnitz, J.C. Butler, et al., *Emerg. Infect. Dis.*, 8 (2002) 1019
17. R.C. Spencer, *J. Clin. Pathol.*, 56 (2003) 182
18. J. A. Jernigan, D.S. Stephens, D. A. Ashford, C. Omenaca, M.S. Topiel, M. Galbraith, et al., *Emerg. Infect. Dis.*, 7 (2001) 933
19. J.R. Uhl, C. A. Bell, L.M. Sloan, M.J. Espy, T.F. Smith, J.E. Rosenblatt, et al., *Mayo Clin. Proc.* 77 (2002) 673
20. J. Kim, M.-Y. Yoon, *Analyst*, 135 (2010) 1182
21. J. Kim, V. Gedi, S.-C. Lee, J.-H. Cho, J.-Y. Moon, M.-Y. Yoon, *Appl. Biochem. Biotechnol.*, 176 (2015) 957
22. F. Patolsky, G. Zheng, O. Hayden, M. Lakadamyali, X. Zhuang, C.M. Lieber, *Proc. Natl. Acad. Sci. U. S. A.*, 101 (2004) 14017.
23. L. Wang, Y. Han, S. Zhou, G. Wang, X. Guan, *ACS Appl. Mater. Interfaces*, 6 (2014) 7334
24. S. Pal, E.C. Alocilja, *Biosens. Bioelectron.*, 26 (2010) 1624
25. K.P. Acharya, A. Erlacher, B. Ullrich, *Thin Solid Films*, 515 (2007) 4066
26. D.W. Branch, S.M. Brozik, *Biosens. Bioelectron.*, 19 (2004) 849
27. F. Lucarelli, G. Marrazza, I. Palchetti, S. Cesaretti, M. Mascini, *Anal. Chim. Acta.*, 469 (2002) 93
28. J.C. Liao, M. Mastali, Y. Li, V. Gau, M. A. Suchard, J. Babbitt, et al., *J. Mol. Diagnostics.*, 9 (2007) 158
29. H. Park, T.J. Park, Y.S. Huh, B.G. Choi, S. Ko, S.Y. Lee, et al., *J. Colloid Interface Sci.*, 350 (2010) 453
30. H. Lee, Y.O. Kang, S. Choi, *Int. J. Electrochem. Sci.*, 9 (2014) 6793–6808
31. S. V. Pereira, F. A. Bertolino, M. A. Fernández-Baldo, G. A. Messina, E. Salinas, M.I. Sanz, et al., *Analyst.*, 136 (2011) 4745
32. M. Regiart, S. V Pereira, V.G. Spotorno, F. A. Bertolino, J. Raba, *Analyst.*, 139 (2014) 4702
33. V.I. Kravtsov, *Russ. J. Electrochem.*, 36 (2000) 1209.
34. C. Ding, F. Zhao, R. Ren, J.-M. Lin, *Talanta*, 78 (2009) 1148
35. S.F. Little, B.E. Ivins, Microbes Infect., 1 (1999) 131
36. L.K. Wolf, Y. Gao, R.M. Georgiadis, *Langmuir*, 20 (2004) 3357.
37. J.M. Song, M. Culha, P.M. Kasili, G.D. Griffin, T. Vo-Dinh, *Biosens. Bioelectron.*, 20 (2005) 2203
38. R.K. Shervedani, S. Pourbeyram, H. Sabzyan, *J. Electroanal. Chem.*, 660 (2011) 37
39. T. Ahuja, V.K. Tanwar, S.K. Mishra, D. Kumar, a M. Biradar, Rajesh, *J. Nanosci. Nanotechnol.*, 11 (2011) 4692.
40. M. Kesik, F.E. Kanik, G. Hizalan, D. Kozanoglu, E.N. Esenturk, S. Timur, L. Toppare, *Polymer*, 54 (2013) 4463
41. A.B. Steel, T.M. Herne, M.J. Tarlov, *Anal. Chem.*, 70 (1998) 4670
42. F.B. Silva, S.N. Vieira, L.R. Goulart, J.F.C. Boodts, A.G. Brito-Madurro, J.M. Madurro, *Int. J. Mol. Sci.*, 9 (2008) 1173
43. V. Reddy, T.S. Ramulu, B. Sinha, J. Lim, R. Hoque, J. Lee, *Int. J. Electrochm. Sci.*, 7 (2012) 11058
44. J. Park, Y. Lee, B.H. Kim, S. Park, *Structure*, 80 (2008) 4986.
45. S. Taufik, N.A. Yusof, T.W. Tee, I. Ramli, *Int. J. Electrochem. Sci.*, 6 (2011) 1880
46. C. Serpi, L. Kovatsi, S. Girousi, *Anal. Chim. Acta.*, 812 (2014) 26